

## Fast compression and reconstruction of astronomical images based on compressed sensing \*

Wang-Ping Zhou, Yang Li, Qing-Shan Liu, Guo-Dong Wang and Yuan Liu

School of Information and Control, Nanjing University of Information Science & Technology, Nanjing 210044, China; [wpzhou@nuist.edu.cn](mailto:wpzhou@nuist.edu.cn)

Received 2013 November 3; accepted 2014 February 14

**Abstract** With the fast increase in the resolution of astronomical images, the question of how to process and transfer such large images has become a key issue in astronomy. We propose a new real-time compression and fast reconstruction algorithm for astronomical images based on compressive sensing techniques. We first reconstruct the original signal with fewer measurements, according to its compressibility. Then, based on the characteristics of astronomical images, we apply Daubechies orthogonal wavelets to obtain a sparse representation. A matrix representing a random Fourier ensemble is used to obtain a sparse representation in a lower dimensional space. For reconstructing the image, we propose a novel minimum total variation with block adaptive sensing to balance the accuracy and computation time. Our experimental results show that the proposed algorithm can efficiently reconstruct colorful astronomical images with high resolution and improve the applicability of compressed sensing.

**Key words:** methods: data analysis — methods: numerical — techniques: image processing

### 1 INTRODUCTION

We can directly infer properties about outer space through astronomical images, which can be obtained in two ways: ground-based telescopes and space-based telescopes (Hao 2007). With the development of technology, the quantity and quality of astronomical images has rapidly increased, so that it is hard to obtain a large compression ratio with conventional compression techniques. As a result, the question of how to process and transfer such large images has become a key issue in astronomy.

The conventional compression techniques applied to astronomical images can be divided into four categories: the DCT based method (Furht 1995), the wavelet based method (Li et al. 2008; Taubman & Zakhor 1994; Press 1992), the block based fractal compression method (Fisher 1994) and some other methods, such as the multi-resolution Pyramidal Median Transform (PMT) algorithm (Starck et al. 1996) and MathMorph (Huang & Bijaoui 1991). However, it is difficult for all of these methods to achieve large compression ratios with acceptable loss. In addition, computation is an enormous burden for CPUs running these algorithms (Bobin et al. 2008).

---

\* Supported by the National Natural Science Foundation of China.

In recent years, a new sampling theory called compressed sensing (CS) (Candès & Tao 2006; Donoho 2006) has attracted considerable attention. CS recovers the signal from far fewer samples than traditional methods and relies on the sparsity of the signal. CS has been applied to astronomical image processing, but most of these studies have concentrated on the feasibility of CS. Liu et al. (2010) used random and sparse Fourier samples to greatly reduce the amount of measurement samples, and lower the requirements of cost and complexity in telescope systems that rely on Fourier transforms for effective rapid imaging. Kolev presented a simple CS method in the orthogonal wavelet domain (Kolev 2011). His analysis shows that these types of wavelets, such as Symmlet, Daubechies and Coiflet, are especially effective for noise removal. Bobin et al. (2008) treated CS as a new framework to handle multiple observations in the same field of view and recover information at a very low signal-to-noise ratio, which is impossible with standard compression methods. Barbey et al. (2011) successfully applied CS to real Herschel/PACS data, taking account of all the instrumental effects, and significantly improved the resolution of sky maps.

In this paper, we propose a new algorithm for real-time compression and fast reconstruction that can be applied to astronomical images using CS techniques. Inspired by Bobin's research on compression techniques and Gan's block compressed sensing (Gan 2007), we first reconstruct the original signal with fewer measurements. Daubechies orthogonal wavelets are then applied to obtain the sparse representation according to the characteristics of astronomical images. For the process of compression, we design a matrix representing a random Fourier ensemble to obtain a sparse representation of images in a lower dimensional space to improve the quality of reconstructed images. In contrast to iterative hard thresholding with an equivalent measurement matrix, a novel minimum total variation with block adaptive sensing is put forward to balance the accuracy and computation time in the process of image reconstruction. Our experiments demonstrate that the proposed algorithm can improve the image accuracy and calculation speed in real time, which are disadvantages of traditional methods such as iterative thresholding reconstruction.

Section 2 describes the construction process of our minimum total variation with block adaptive sensing method. Section 3 gives experimental results of the proposed method, and compares them to the iterative thresholding and the block TV minimization algorithms. Section 4 provides conclusions.

## 2 BLOCK ADAPTIVE SAMPLING COMPRESSED SENSING FOR ASTRONOMICAL IMAGES

### 2.1 Background

Inspired by the idea from CS that the sparsity of a signal is an a priori condition for compressed sampling, an astronomical image  $I(m, n)$ ,  $m = 1, 2, \dots, M$ ;  $n = 1, 2, \dots, N$  with size  $M \times N$ , can be represented sparsely in a certain basis,

$$I = \psi\alpha, \quad (1)$$

where  $\psi$  is a sparse basis and  $\alpha$  is a sparse matrix representation of  $I$  where most of its coefficients are zero or approximately zero, so that  $\alpha$  is compressive. We choose Daubechies wavelets as the basis, referring to Kolev (2011).

When sampling from  $I$ , the measurement matrix  $\Phi$  must satisfy the RIP condition (Candès & Tao 2006). This means that  $\Phi$  is not related to  $\alpha$ .

$$y = \Phi I \Rightarrow y = \Phi\psi\alpha. \quad (2)$$

Although general random Gaussian matrices have nearly no relation with any other sparse signal, their randomness needs a huge storage space. Meanwhile, the absence of structure in  $\Phi$  makes computing it very complex (Li & Wei 2009). Thus, it is difficult to compute a fast reconstruction of large

scale astronomical images to satisfy practical demands. To handle this issue, we select a fast sensing matrix (random Fourier ensemble) to offer both fast encoding and fast decoding techniques,

$$\Phi = SF, \quad (3)$$

where  $F \in \mathbb{R}^{N \times N}$  is the real Discrete Fourier Transform and the matrix  $S \in \mathbb{R}^{t \times N}$  randomly selects a few elements of any  $N$ -dimensional vector. The random Fourier measurement reduces the complexity of the sampling system (Jacques & Vandergheynst 2010).

The solution to the reconstruction problem is achieved by solving the following convex problem,

$$\hat{\alpha} = \arg \min \|\alpha\|_1 \quad \text{s.t.} \quad y = \Phi\psi\alpha. \quad (4)$$

In practical applications, astronomical images are often obtained in a noisy environment, for example, where cosmic radiation is present, so a more realistic CS model should take account of noise given by the expression  $y = \Phi(I + \eta)$ , where  $\eta$  represents noise. Then, a relaxed version becomes

$$\hat{\alpha} = \arg \min \|\alpha\|_1 \quad \text{s.t.} \quad \|y - \Phi\psi\alpha\|_2 \leq \varepsilon. \quad (5)$$

There are several methods to solve Equation (5), such as stagewise orthogonal matching (Donoho et al. 2012), gradient projection (Figueiredo et al. 2007) and iterative hard thresholding (Gan 2007; Bobin et al. 2008).

## 2.2 Total Variation Minimization

Bobin and Gan reconstructed an image with iterative hard thresholding. Compared with the former two methods, iterative hard thresholding has a faster construction speed. However, it is sensitive to the initial thresholds, and the sparse solution is only optimized in the local parameter space.

In this paper, we aim at improving the quality of reconstruction and increasing the speed of computation. The total variation (TV) minimization method is designed to reconstruct  $I$  from another angle, in which the images are compressible with respect to their discrete gradient. Concretely, we denote  $I_{m,n}$  as any particular pixel of  $I$ . The discrete gradients  $D_1 I_{m,n}$  and  $D_2 I_{m,n}$  are defined as

$$\begin{cases} D_1 I_{m,n} = I_{m+1,n} - I_{m,n} \\ D_2 I_{m,n} = I_{m,n+1} - I_{m,n} \end{cases}. \quad (6)$$

The TV is the sum of magnitudes of the discretized gradient

$$\|I\|_{\text{TV}} = \sum \sqrt{(D_1 I)^2 + (D_2 I)^2} = \sum |(\nabla I)_{m,n}|. \quad (7)$$

Accordingly, the model for reconstruction is changed to

$$(\text{TV}) \min \|I\|_{\text{TV}} \quad \text{s.t.} \quad \|AI - y\|_2 \leq \varepsilon, \quad (8)$$

where  $A = \Phi\psi^{-1}$ . Through TV minimization, the result is exact and robust (Needell & Ward 2013). However, model (8) can be converted to an unconstrained convex problem.

$$\text{minimize } \|AI - y\|_2^2 + \lambda \|I\|_{\text{TV}}, \quad (9)$$

where the parameter  $\lambda > 0$  acts as a tradeoff between the sparsity of  $I$  and the approximation error. To describe this method, we should define the matrix pairs  $(p, q)$  as  $\varrho$ , where  $p \in R^{(M-1) \times N}$  and  $q \in R^{M \times (N-1)}$  satisfy

$$\begin{aligned} p_{m,n}^2 + q_{m,n}^2 &\leq 1, & \text{for } 1 \leq m \leq M-1, 1 \leq n \leq N-1, \\ |p_{m,M}| &\leq 1, & \text{for } 1 \leq m \leq M-1, \\ |q_{n,N}| &\leq 1, & \text{for } 1 \leq n \leq N-1. \end{aligned} \quad (10)$$

A linear operator  $\Gamma$  maps the element of  $\varrho$  to an  $M \times N$  matrix as

$$[\Gamma(p, q)]_{m,n} = p_{m,n} - p_{m-1,n} + q_{m,n} - q_{m,n-1}, \quad \text{for } 1 \leq m \leq M, 1 \leq n \leq N. \quad (11)$$

Finally, the algorithm is outlined below.

Inputs: observed image  $I$ , regularization parameter  $\lambda$  and iteration number  $J$ .

Output: An optimal solution  $I^*$  of (9) up to tolerance.

Step 0: Take  $(p_0, q_0) = [O_{(m-1) \times n}, O_{m \times (n-1)}]$ .

Step  $j$  ( $j = 1, 2, \dots, J$ ): Compute

$$(p_j, q_j) = P_\varrho \left\{ (p_{j-1}, q_{j-1}) + \frac{1}{4\lambda} \Gamma^T \left[ I - \lambda \Gamma(p_{j-1}, q_{j-1}) \right] \right\} \quad (12)$$

Set  $I^* = P_{B_{t,u}} \left[ I - \lambda \Gamma(p_J, q_J) \right]$ .

The projection operator  $P_\varrho$  in (12) maps a matrix pair  $(p, q)$  to another matrix pair  $(r, s) = P_\varrho(p, q)$ .

### 2.3 Block Adaptive Sampling

The TV minimization algorithm also suffers from fairly heavy computations. Motivated by the great success of the block DCT coding system, block CS is proposed in Gan (2007). In the block CS framework, an image is divided into small blocks  $I_{u,v}$  with the same size of  $B \times B$  and with the same measurement operator  $\Phi_b$ . The corresponding output sensing result can be represented by

$$y_{u,v} = \Phi_b I_{u,v}. \quad (13)$$

So, for the entire image, the measurement matrix can be written in a block diagonal form

$$\Phi = \begin{bmatrix} \Phi_b & & & \\ & \Phi_b & & \\ & & \ddots & \\ & & & \Phi_b \end{bmatrix}. \quad (14)$$

Due to the different sparsities of different blocks, there is a drawback if all the blocks are sampled with the same operator. If the  $i$ th block has a very low sparsity and the number of measurements is too large, it will result in a waste of resources; Or, if the sparsity of the block is relatively high, lower sampling will affect accuracy of reconstruction and generate some intermittent visual errors. So, we propose a Block Adaptive Sampling TV minimization algorithm (BASTV), which considers the different sparsities of different blocks, while  $I_{u,v}$  is measured with different sensing matrices.

In BASTV, the first block  $I_1$  is treated as a reference, and its sensing matrix should satisfy  $S_1 \geq k_1 \log P_1$ , where  $P_1$  stands for the sum of the pixels in the first image block and its sparsity is represented by  $k_1$ . After this, we can compute the sampling rate of the  $i$ th block based on  $I_1$  by  $S_i = S_1 k_i / k_1$ , where  $k_i$  is the sparsity of the  $i$ th block. Sparsity  $k$  is the proportion of nonzero elements in the matrix.

For an image acquired during observations, its edge information often reflects the sparsity in the transformed domain. More edge points mean more saltation is present in the pixel domain and lower sparsity in the transformed domain, so that we can directly judge the sparsity in the pixel domain through image edge detection. Sobel edge detection can be used to analyze the sparsity because of its low computational complexity and excellent performance (Ercan & Whyte 2001). The edge image is transformed into a binary image where 1 stands for edge points and 0 represents non-edge points. Then, we can regard the edge points in each block as the sparsity  $k_i$ .

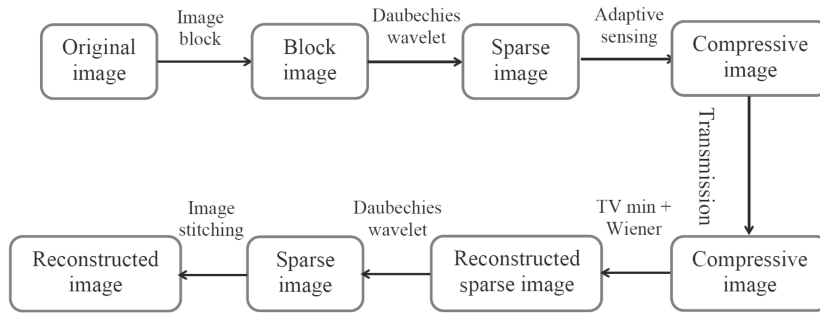


**Fig. 1** The whole process of fast compression and reconstruction of astronomical images in the CS framework.

Finally, the adaptive sampling operation can be represented as

$$\tilde{\Phi} = \begin{bmatrix} \tilde{\Phi}_1 & & & \\ & \tilde{\Phi}_2 & & \\ & & \ddots & \\ & & & \tilde{\Phi}_B \end{bmatrix}. \tag{15}$$

Thus, the proposed adaptive sensing guarantees the accuracy of reconstruction and at the same time ensures a judicious use of resources.

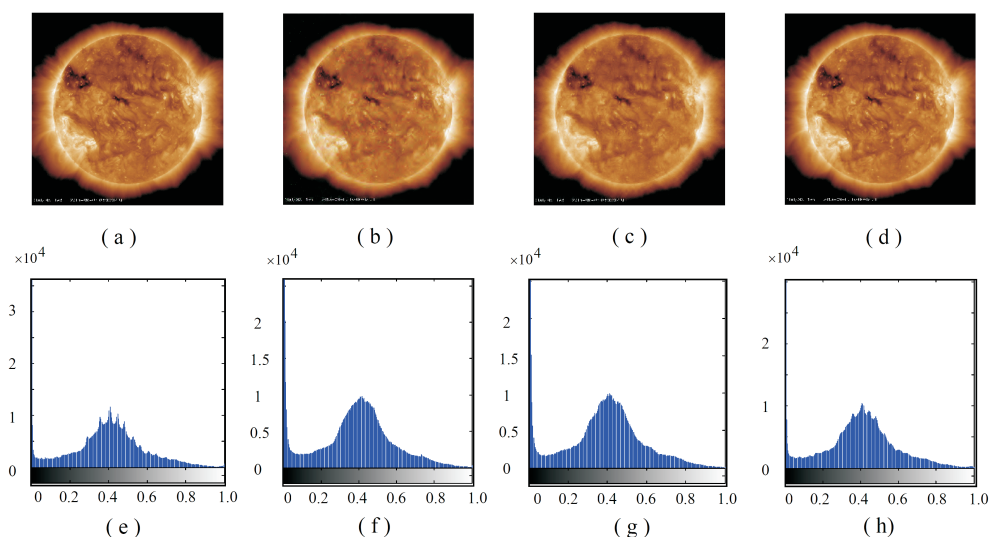
As described in Gan (2007), the block dimension  $B = 32$  is suggested and a  $3 \times 3$  Wiener filter is applied in the spatial domain to reduce the blocking artifact and smooth the reconstructed image. The process of fast compression and reconstruction in a CS frame is demonstrated in Figure 1.

### 3 EXPERIMENTAL RESULTS

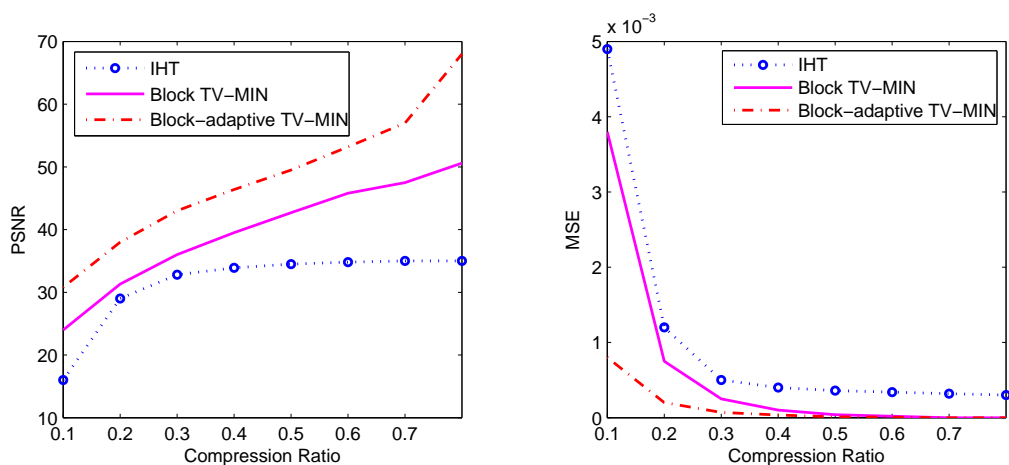
To investigate the performance of the proposed TV minimization method that uses block adaptive sensing, we compare it to the iterative thresholding method (Bobin et al. 2008) and the block TV minimization method (Gan 2007). Unlike previous work that has conducted experiments on gray-level images, we tested our method on a colorized Sun image with size  $1024 \times 1024$  for practical application, which is available online at the Solar Dynamics Observatory (SDO) website, and classic color images of galaxies, nebulae, stars and the Universe, which were obtained from the Hubble Space Telescope. Because the three color channels R, G and B are highly correlated, the result of each channel processed separately is unnecessary. To enhance the effect of color image reconstruction, channel R is selected as a reference. We can then get  $G'$  and  $B'$  through averaging G and B with R to achieve compression. The experiments are implemented on a PC with an Intel Core i7 3.4 GHz CPU and 16 GB of RAM, Windows 7 and Matlab R2011b.

In Figure 2, each image is reconstructed with a 30% sensing rate and the gray level histogram for the corresponding image is shown. Visually, the BASTV algorithm performs well because it provides a solution that is close to the original image. The sharpness of the reconstructed image is better than the other two methods. The objective quality of the reconstructed images is also measured by PSNR. For a color image, computation of PSNR is defined as

$$\text{PSNR} = 10 \log \frac{255^2}{\frac{1}{MN} \left\{ \sum_j^3 \sum_{m=1}^M \sum_{n=1}^N [I_j(m, n) - \hat{I}_j(m, n)]^2 \right\} / 3}, \tag{16}$$



**Fig. 2** (a)–(d): original SDO image, reconstructed image by IHT, reconstructed image by BTV–min, reconstructed image by BASTV–min; (e)–(h): gray level histogram corresponding to (a)–(d).

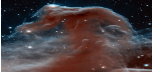


**Fig. 3** PSNR increasing and MSE decreasing with the growth of the measurement rate for each image.

where  $M$  and  $N$  denote the rows and columns of the image, respectively.  $j = 1, 2, 3$  stand for the three channels in the color image, respectively. Various sensing ratios are used to validate the effectiveness of the proposed method. We conducted eight tests for each image at different measurement rates.

Figure 3 illustrates that the PSNR values increase and MSE values decrease with the growth of the measurement rate for each image. For the iterative thresholding method, PSNR does not increase after a sensing rate of 30%. It can be seen that the BASTV algorithm has the best performance at

**Table 1** PSNR of Different Images Sampled with Different Ratios

		10%	20%	30%	40%	50%
 Galaxy	IHT	20.5808	35.2554	38.1166	39.4995	40.0967
	BTV-min	29.7142	35.2244	39.9649	42.6330	45.1968
	BASTV-min	39.0203	45.1729	42.6330	52.4919	45.1968
 Nebula	IHT	17.2873	25.6129	28.8608	30.1763	30.6656
	BTV-min	22.5588	26.7596	30.6449	33.9150	37.1294
	BASTV-min	24.8311	30.1785	34.5977	37.9639	40.9334
 Universe	IHT	18.0158	26.1572	27.8563	28.8514	29.4639
	BTV-min	25.5546	28.1134	30.1061	31.8241	34.2992
	BASTV-min	26.2880	28.9967	31.0337	33.2671	35.9946
 Star	IHT	19.3212	26.3095	30.3701	31.5605	31.9855
	BTV-min	22.8690	26.4708	30.4033	33.6947	37.3234
	BASTV-min	24.5558	29.6246	34.8599	38.2334	41.4402

**Table 2** Comparison of Reconstruction Methods under Different Kinds of TV-min

Reconstruction Method		10%	20%	30%
MSE	TV-MIN	0.0011	8.6037e-005	3.3204e-005
	Block TV-MIN	0.0039	7.8665e-004	2.6570e-004
	Block adaptive TV-MIN	0.3259e-004	0.3259e-004	0.3259e-004
PSNR	TV-MIN	29.5656	40.6532	44.7882
	Block TV-MIN	24.0569	31.0422	35.7561
	Block adaptive TV-MIN	30.7957	37.9421	42.7255
Time/s	TV-MIN	276.0863	285.7559	283.9373
	Block TV-MIN	207.6559	192.3176	189.1788
	Block adaptive TV-MIN	203.8339	193.0413	189.5080

different rates. The PSNR values for different kinds of astronomical images sampled with different ratios are reported in Table 1.

Obviously, for these reconstructed images, BASTV-min always yields a higher PSNR than the other two methods. Furthermore, we report the computation cost of the proposed algorithm in Table 2.

From the above table, we can see that the block TV minimization obviously improves the reconstruction speed, but reduces the correlation of the whole image, so as to reduce the accuracy of reconstruction. The inclusion of the BASTV algorithm and deblocking filters makes up for the lack of TV-min. That maintains the balance between speed and accuracy during reconstruction.

#### 4 CONCLUSIONS

A block adaptive sensing TV-min method was proposed for astronomical images in the CS frame, which aimed at achieving real-time sampling compression and fast reconstruction for astronomy.

We selected Daubechies wavelets for better sparsity and a random Fourier ensemble for lower complexity for sampling the system. During reconstruction, the block adaptive sensing TV–min method maintained a balance between speed and accuracy during reconstruction. The experimental results indicated that the proposed method was very efficient in terms of PSNR, visual quality and reconstruction speed.

**Acknowledgements** This work was funded by the National Natural Science Foundation of China (Grant No. 11322329), and the foundation of the Priority Academic Program Development (PAPD) of Jiangsu Higher Education Institutions.

## References

- Barbey, N., Sauvage, M., Starck, J.-L., Ottensamer, R., & Chanial, P. 2011, *A&A*, 527, A102
- Bobin, J., Starck, J.-L., & Ottensamer, R. 2008, *IEEE Journal of Selected Topics in Signal Processing*, 2, 718
- Candès, E. J., & Tao, T. 2006, *Information Theory, IEEE Transactions on*, 52, 5406
- Donoho, D. L. 2006, *Information Theory, IEEE Transactions on*, 52, 1289
- Donoho, D. L., Tsai, Y., Drori, I., & Starck, J. L. 2012, *Information Theory, IEEE Transactions on*, 58, 1094
- Ercan, G., & Whyte, P. 2001, *Digital image processing*, US Patent 6, 240, 217 (Google Patents)
- Figueiredo, M. A. T., Nowak, R. D., & Wright, S. J. 2007, *IEEE Journal of Selected Topics in Signal Processing*, 1, 586
- Fisher, Y. 1994, *Fractal Compression: Theory and Application to Digital Images* (New York: Springer Verlag)
- Furht, B. 1995, *Real-Time Imaging*, 1, 319
- Gan, L. 2007, in *Digital Signal Processing, 2007 15th International Conference on*, 403–406 (IEEE)
- Hao, Z.-X. 2007, *Morden Scientific Instruments*, 05, 543
- Huang, L., & Bijaoui, A. 1991, *Experimental Astronomy*, 1, 311
- Jacques, L., & Vandergheynst, P. 2011, *Compressed Sensing: “When Sparsity Meets Sampling”*, in *Optical and Digital Image Processing: Fundamentals and Applications*, eds. G. Cristobal, P. Schelkens, & H. Thienpont (Germany, Weinheim: Wiley-VCH Verlag GmbH & Co. KGaA)
- Kolev, V. 2011, arXiv:1111.6276
- Li, L., Dai, H.-B., & Xu, J. 2008, *Astronomical Research and Technology*, 5, 380
- Li, S.-T., & Wei, D. 2009, *Acta Automatica Sinica*, 35, 1369
- Liu, X. Y., Dong, L., & Wang, J. L. 2010, *Optics and Precision Engineering*, 3, 005
- Needell, D., & Ward, R. 2013, *SIAM Journal on Imaging Sciences*, 6, 1035
- Press, W. H. 1992, in *Astronomical Society of the Pacific Conference Series*, 25, *Astronomical Data Analysis Software and Systems I*, eds. D. M. Worrall, C. Biemesderfer, & J. Barnes, 3
- Starck, J.-L., Murtagh, F., Pirenne, B., & Albrecht, M. 1996, *PASP*, 108, 446
- Taubman, D., & Zakhor, A. 1994, *IEEE Transactions on Image Processing*, 3, 572